

hep-lat/9509002

AZPH-TH/95-22

October 17, 2018

High density QCD with static quarks

Thomas C. Blum¹

tblum@physics.arizona.edu

James E. Hetrick

hetrick@physics.arizona.edu

Doug Toussaint

toussaint@physics.arizona.edu

*Department of Physics
University of Arizona
Tucson, AZ 85712 USA*

Abstract

We study lattice QCD in the limit that the quark mass and chemical potential are simultaneously made large, resulting in a controllable density of quarks which do not move. This is similar in spirit to the quenched approximation for zero density QCD. In this approximation we find that the deconfinement transition seen at zero density becomes a smooth crossover at any nonzero density, and that at low enough temperature chiral symmetry remains broken at all densities.

¹ Address after 1 Oct. 1995: Brookhaven National Laboratory, Upton, NY 11973

1 Introduction

Lattice QCD with a nonzero density of quarks is a difficult problem due to the fact that the fermion determinant is not a positive real number, and thus cannot be used as a weight for generating configurations by Monte Carlo methods[1]. This is unfortunate since situations with a non-negligible density of quarks are interesting physically, such as the interiors of neutron stars or the dynamics of heavy ion collisions at RHIC. A further technical difficulty is that with Kogut-Susskind quarks the fermion matrix is badly ill-conditioned at nonzero chemical potential[2], making simulations even more difficult. Hence at present, only crude results on very small lattices are available[3, 4]. Because of our inability to deal with the full problem, we may consider approximations which hopefully capture some of the essential features of the physics. Here we present a study of QCD at arbitrary quark density in an approximation where the dynamics of the quarks has been removed. This approximation is then analogous to the quenched approximation at zero density, an approximation which has provided considerable insight into the nature of QCD.

2 Theory

Our idea is to simultaneously take the limits of infinite quark mass and infinite chemical potential in such a way that the density of quarks remains fixed at some value. This leaves us with quarks that can be present or absent at each lattice site, but which do not move in the spatial directions owing to their infinite mass. The result is a much simpler fermion determinant such that gauge variables can be updated to equilibrium in the background of a prescribed density of quarks, with little more difficulty than updating in the quenched approximation.

The general idea of studying the problem in simple approximations is not new. DeGrand and DeTar have studied an extension of the three dimensional Potts model with an imaginary magnetic field, which has similar symmetry breaking as in QCD, and might be expected to lie in the same universality class[5]. Satz has used a lowest order hopping parameter expansion on $8^3 \times 3$ lattices[6], which is also an approach based on very heavy quarks.

With a chemical potential included, the lattice Dirac operator using Kogut-Susskind quarks is

$$M(x, y) = 2am_q\delta_{x,y} + \sum_{\nu=1,2,3} \left[U_\nu(x)\eta_\nu(x)\delta_{x+\hat{\nu},y} - U_\nu^\dagger(y)\eta_\nu(y)\delta_{x-\hat{\nu},y} \right] + \left[e^{\mu a}U_t(x)\eta_t(x)\delta_{x+\hat{t},y} - e^{-\mu a}U_t^\dagger(y)\eta_t(y)\delta_{x-\hat{t},y} \right] \quad (1)$$

This can be written as

$$\begin{pmatrix} \mathbf{B}_0 & e^{\mu a} \mathbf{T}_0 & 0 & \cdots & e^{-\mu a} \mathbf{T}_{n_t}^\dagger \\ -e^{-\mu a} \mathbf{T}_0^\dagger & \mathbf{B}_1 & e^{\mu a} \mathbf{T}_1 & \cdots & \\ 0 & -e^{-\mu a} \mathbf{T}_1^\dagger & \mathbf{B}_2 & & \\ \vdots & \vdots & & \ddots & \\ -e^{\mu a} \mathbf{T}_{n_t} & & & & \end{pmatrix} \quad (2)$$

where \mathbf{B}_i contains the diagonal mass term and all the spatial hopping terms on the i th time slice, and \mathbf{T}_i contains all the time direction hoppings from slice i to slice $i + 1$.

We now take the limits $m \rightarrow \infty$ and $\mu \rightarrow \infty$ simultaneously. This leaves us with $2ma$ along the diagonal, and the forward hopping terms, $e^{\mu a} \mathbf{T}_i$. Each spatial point is decoupled from all others, and the fermion determinant is just a product of easily computed determinants on each static worldline:

$$\det(M) = \prod_{\vec{x}} e^{\mu a n_c n_t} \det(P_{\vec{x}} + C \mathbf{1}). \quad (3)$$

Here $P_{\vec{x}}$ is the Polyakov loop at spatial site \vec{x} , n_c is the number of colors, and n_t is the number of time slices. The coefficient of the unit matrix, C , is $(2ma/e^{\mu a})^{n_t}$, and is the fundamental parameter in our approximation, through which we fix the density (We will see later that C^{-3} is the ratio of the probability that there are three quarks (in SU(3)) on a site to the probability that the site is empty.).

The determinant is easily evaluated by diagonalizing $P_{\vec{x}}$. In SU(2),

$$\det(P_{\vec{x}} + C) = C^2 + C \operatorname{Tr} P_{\vec{x}} + 1, \quad (4)$$

while in SU(3)

$$\det(P_{\vec{x}} + C) = C^3 + C^2 \operatorname{Tr} P_{\vec{x}} + C \operatorname{Tr} P_{\vec{x}}^* + 1. \quad (5)$$

In SU(2) this determinant is real and positive, which reflects the fact that quarks and antiquarks are in equivalent representations of SU(2). Unfortunately, studying SU(2) at large baryon density is of limited interest since such baryons would be bosons. Neutron stars would be quite different in this case as would supernovae. In the realistic case of SU(3), we are still left with a complex determinant, albeit a much simpler one, allowing us to generate high statistics.

In generating gauge configurations, the determinant in the partition function is written as the exponential of a sum over spatial sites

$$Z = \int [dU] \prod_{\vec{x}} e^{\mu a n_t n_c} \det(P_{\vec{x}} + C) e^{-S_g}$$

$$= \int [dU] e^{-S_g + \sum_{\vec{x}} \left\{ \mu a n_t n_c + \ln [\det(P_{\vec{x}} + C)] \right\}}. \quad (6)$$

We can update the spatial links with any of the standard algorithms for quenched QCD: Metropolis, heat bath and/or overrelaxation. The temporal links are updated with the Metropolis algorithm, using the magnitude of the determinant plus the gauge action as the weight. Thus the parts of the action involved in updating a temporal link U_t are

$$S = \dots + (2/g^2) \text{Re Tr } U_t \tilde{S} + \log \left(\left| \det(U_t \tilde{P}_{\vec{x}} + C) \right| \right) + \dots \quad (7)$$

where \tilde{S} is the sum of the ‘‘staples’’ and $\tilde{P}_{\vec{x}}$ is the product of all the time direction links at site \vec{x} except for the link being updated. As in conventional quenched QCD, successive Metropolis hits are easy; most of the work goes into evaluating the staples and $\tilde{P}_{\vec{x}}$ which can be used unchanged in successive hits.

Because of the phase in the determinant, for SU(3) we must estimate expectation values by taking the ratio

$$\langle \mathcal{O} \rangle = \frac{\langle \mathcal{O} e^{i\theta} \rangle_{\parallel}}{\langle e^{i\theta} \rangle_{\parallel}} \quad (8)$$

where θ is the phase of the determinant summed over all spatial points and $\langle \rangle_{\parallel}$ indicates an expectation value in the ensemble of configurations weighted by the magnitude of the determinant. This method can be applied to the full theory; however the expectation value of the phase can (and typically does) become very small, so that enormous statistics are required to get meaningful measurements. In our case the phase does become small, however not prohibitively so on the lattices we study (our smallest value was $\langle e^{i\theta} \rangle_{\parallel} = 0.02$). Furthermore, as described above, we can produce statistics generously.

The physical quark density is obtained from

$$\begin{aligned} \langle n \rangle &= \frac{1}{\beta V} \frac{\partial \ln(Z)}{\partial \mu} \\ &= \frac{1}{\beta V} \left\langle \sum_{\vec{x}} \left\{ a n_t n_c + \left(\frac{\partial C}{\partial \mu} \right) \left(\frac{\partial \ln(\det(P_{\vec{x}} + C))}{\partial C} \right) \right\} \right\rangle \end{aligned} \quad (9)$$

where V is the spatial volume and $\beta = a n_t$ is the temporal extent of the lattice. Using equations 4 and 5 this becomes

$$\langle n \rangle = \frac{1}{V} \left\langle \sum_{\vec{x}} \frac{C T_{\vec{x}} + 2}{C^2 + C T_{\vec{x}} + 1} \right\rangle \quad (10)$$

in SU(2), and

$$\langle n \rangle = \frac{1}{V} \left\langle \sum_{\vec{x}} \frac{C^2 T_{\vec{x}} + 2 C T_{\vec{x}}^* + 3}{C^3 + C^2 T_{\vec{x}} + C T_{\vec{x}}^* + 1} \right\rangle \quad (11)$$

in SU(3), where $T_{\vec{x}} = \text{Tr}(P_{\vec{x}})$. At $C = \infty$ the density is 0; at $C = 0$ the system is saturated with density n_c per site; $C = 1$ represents “half-filling” and the density is $n_c/2$.

Note from Eqs. 4 and 5 that $\det(P_i + C)$ is unchanged by the replacement $C \rightarrow 1/C$, where in SU(3) we simultaneously replace $U \rightarrow U^*$. Thus there is a duality relation: the ensemble of configurations generated with coupling C is the same as that generated at coupling $1/C$, and the density obeys $\rho(1/C) = n_c - \rho(C)$. Physically this duality reflects the fact that $n_c - 1$ quarks on a single site behave like an antiquark on that site, so that the system nearly saturated with quarks, or equivalently a quark saturated system with a small density of holes behaving as antiquarks (at small C), behaves the same as a system with a small density of quarks (at large C).

Alternatively, we may wish to know the probability that a site contains zero, one, two, or three (in SU(3)) quarks. Imagine separating the partition function into sectors with a fixed number of quarks on the particular site in question. These sectors are distinguished by their dependence on the chemical potential

$$Z = Z_0 + e^{\mu_{ant}t} Z_1 + e^{2\mu_{ant}t} Z_2 + e^{3\mu_{ant}t} Z_3. \quad (12)$$

The fermion determinant at site \vec{x} introduces (Eqs. 3 and 5) a factor of

$$e^{3\mu_{ant}t} \left(C^3 + C^2 T_{\vec{x}} + C T_{\vec{x}}^* + 1 \right) \quad (13)$$

into the integrand of the partition function, and C contains a factor of $e^{-\mu_{ant}t}$. Thus the probabilities of finding given numbers of quarks at site \vec{x} are just given by the individual terms in this polynomial in C :

$$\begin{aligned} p_0(\vec{x}) &= \left\langle \frac{C^3}{C^3 + C^2 T_{\vec{x}} + C T_{\vec{x}}^* + 1} \right\rangle \\ p_1(\vec{x}) &= \left\langle \frac{C^2 T_{\vec{x}}}{C^3 + C^2 T_{\vec{x}} + C T_{\vec{x}}^* + 1} \right\rangle \\ p_2(\vec{x}) &= \left\langle \frac{C T_{\vec{x}}^*}{C^3 + C^2 T_{\vec{x}} + C T_{\vec{x}}^* + 1} \right\rangle \\ p_3(\vec{x}) &= \left\langle \frac{1}{C^3 + C^2 T_{\vec{x}} + C T_{\vec{x}}^* + 1} \right\rangle \end{aligned} \quad (14)$$

Note, the probability to find either zero, one, two, or three quarks is normalized to one for each configuration. We see from Eqs. 14 that the ratio of the probability of three quarks on a site to the site being empty is just C^{-3} . However, the value of C does not *a priori* determine the density, since the probabilities of one or two quarks on a site depend on the dynamics. Similarly we may calculate correlation functions $\langle p_n(\vec{x}) p_m(\vec{y}) \rangle$, the probability for

n quarks at site \vec{x} and m quarks at site \vec{y} , such as

$$p_{11}(\vec{x} - \vec{y}) = \left\langle \left(\frac{C^2 T_{\vec{x}}}{C^3 + C^2 T_{\vec{x}} + C T_{\vec{x}}^* + 1} \right) \left(\frac{C^2 T_{\vec{y}}}{C^3 + C^2 T_{\vec{y}} + C T_{\vec{y}}^* + 1} \right) \right\rangle, \quad (15)$$

etc. These correlations may be used to study the clustering properties of baryons in the model as temperature and density are varied.

Since in our approximation the only remaining combination of chemical potential and quark mass is C , the heavy quark condensate $\langle \bar{\Psi}\Psi \rangle = \frac{1}{\beta V} \frac{\partial \ln(Z)}{\partial m}$ is trivially related to $\langle n \rangle$. However we use $\langle \bar{\psi}\psi \rangle$ evaluated for light quarks on the generated lattices as an indicator of chiral symmetry breaking. This is just a probe of the nature of the gauge configurations, rather than a condensate of the actual quarks in the model. It represents the chiral properties of light valence quarks in the presence of a finite density of massive quarks.

We can also calculate the average Polyakov loop. Not surprisingly, since the heavy quarks are coupled directly to the Polyakov loop, it gets a nonzero expectation value at any C other than zero or infinity. This does not necessarily represent deconfinement, since we have put in a density of quarks which can now shield the test quark represented by the Polyakov loop.

3 Simulation Results

Below we describe results for both SU(2) and SU(3) gauge groups; it is interesting to compare the two symmetries, since the nature of the phase transition is rather different in each. For pure SU(2) gauge theory the high temperature transition at zero density is second order [7], so we expect smooth behavior as the density is varied away from this point. For pure SU(3) (or quenched QCD), the high temperature transition is first order [8], and we expected this behavior to extend into the interior of the $T-\mu$ phase diagram. Surprisingly, we find this is apparently not the case. The first order transition appears to become a crossover at non-zero density, becoming quite smooth at relatively low densities.

3.1 SU(2)

Our initial studies were done in SU(2) where we ran at a two values of the gauge coupling, $4/g^2 = 1.5$ and 2.0 while varying the parameter C between zero and one. This actually corresponds to varying the density of “antiquarks” (holes relative to a quark saturated lattice) from zero to one per site, but as mentioned earlier, the physics is the same as for quarks.

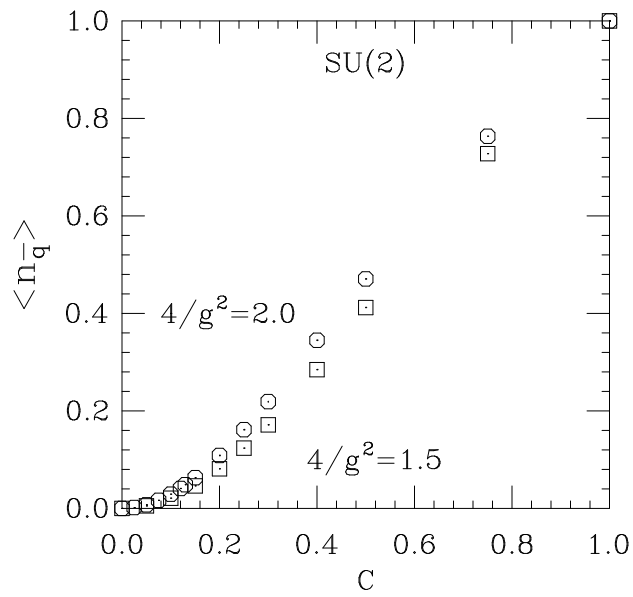


Figure 1: The expectation of the density for SU(2) given by Eq. 10. $C = 0$ corresponds to zero density of antiquarks, and $C = 1$ corresponds to one antiquark per site.

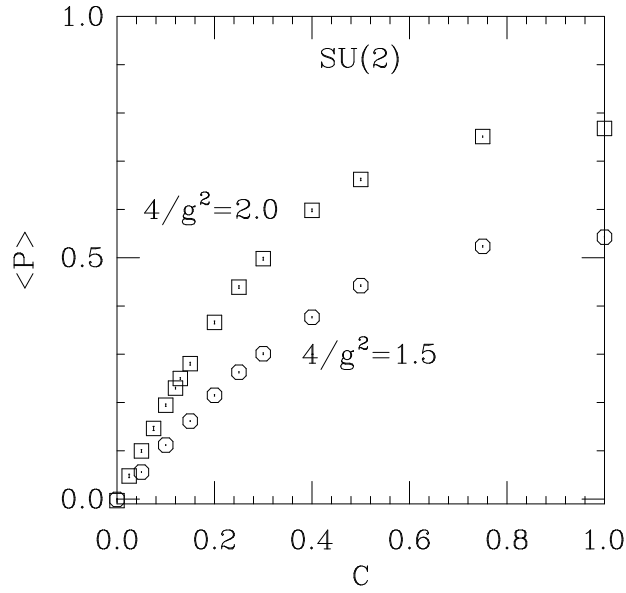


Figure 2: The magnitude of the Polyakov loop for SU(2) and the dense static quark action given in Eq. 6. The nonzero value of the Polyakov loop is due to its explicit coupling to C in the action and does not necessarily indicate deconfinement.

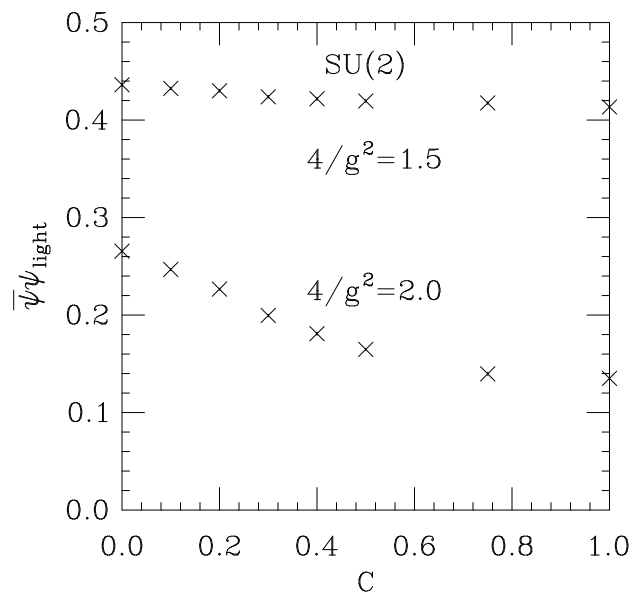


Figure 3: The light quark $\langle \bar{\psi}\psi \rangle$ found by inverting the usual Kogut-Susskind fermion matrix on gauge configurations generated with the dense static quark action given in Eq. 6. The light quark mass is 0.025, and we have normalized to two flavors.

The second value of the gauge coupling is near the $n_t = 4$ zero density temperature driven transition which is at roughly $4/g^2 \approx 2.3$, while the first corresponds to a much lower temperature. The simulations were done on $8^3 \times 4$ lattices.

In Figs. 1 and 2 we show the density of antiquarks and the magnitude of the Polyakov loop as a function of the parameter C . As expected, both exhibit smooth behavior. In Fig. 3 we show the light quark $\langle \bar{\psi}\psi \rangle$ (normalized to two flavors) using Kogut-Susskind quarks with $am_q = 0.025$ for various values of the density. For $4/g^2 = 2.0$ (near the zero density transition) $\langle \bar{\psi}\psi \rangle$ shows a smooth decrease to a minimum that is roughly one half the zero density value. However, on the colder lattice there is only a slight decrease in $\langle \bar{\psi}\psi \rangle$. Since the light quark $\langle \bar{\psi}\psi \rangle$ is measuring the density of near zero eigenvalues of the light quark hopping matrix, this amounts to saying that for cold enough lattices a high density of static quarks does not suffice to remove the disorder in the gauge fields found at zero density.

3.2 SU(3)

We have run on $6^3 \times 2$, $8^3 \times 2$, $10^3 \times 2$, and $6^3 \times 4$ lattices. Typical runs include 500 equilibration sweeps of the lattice and 4000 measuring sweeps, where in each sweep we make two overrelaxation updates of the spatial links and ten Metropolis updates of both spatial and temporal links. The average phase on the $n_t = 2$ lattices ranges from one, at $1/C = 0.0$, to as small as 0.04 (the $10^3 \times 2$ lattice at $6/g^2 = 4.8$ and $1/C = 0.08$). Since all physical observables are obtained from a ratio of expectation values (Eq. 8) where the numerator and denominator are strongly correlated, we use a jackknife procedure with ten blocks to estimate the errors.

In Figs. 4 and 5 we summarize the behavior of the density and Polyakov loop magnitude ($|P|$) in the $T-\mu$ plane, on $N_t = 2$ lattices. Fig. 4 shows $\langle n \rangle$ as a function of $6/g^2$ (temperature) and $1/C$ (effectively μ). In Fig. 5 at $1/C = 0$, or zero density, we see the strong first order temperature induced transition at $6/g^2 \approx 5.1$ in $|P|$. As the density increases, this transition smooths out.

Figs. 6, 7 and 8 show the density, $|P|$ and light quark $\langle \bar{\psi}\psi \rangle$ along lines of constant $1/C$ on $6^3 \times 2$, $8^3 \times 2$ and $10^3 \times 2$ lattices. From these plots, it appears that the first order transition at $1/C = 0$ becomes a smooth crossover for any nonzero value of the density. This is surprising, since conventional wisdom says that a nonzero discontinuity at the edge of a phase diagram decreases continuously to zero at some point in the interior of the phase diagram. However, we note that simple functions such as $\tanh(\frac{t-t_c}{h^x})$ have a discontinuity at $h = 0$ but a crossover at any nonzero h . Since we see no systematic dependence of the

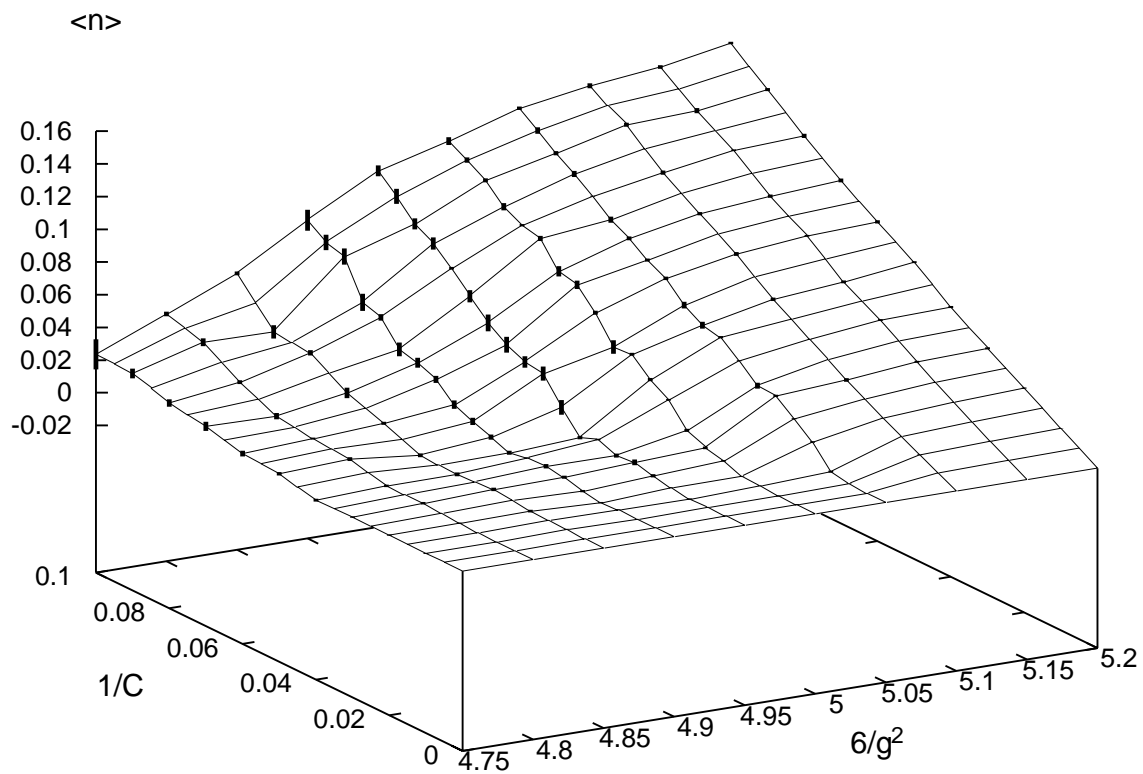


Figure 4: The quark density in SU(3) for $n_t = 2$ as a function of $6/g^2$ and $1/C$. Note that the density is always zero at $1/C = 0$. This plot includes results from $6^3 \times 2$, $8^3 \times 2$ and $10^3 \times 2$ lattices. In the smoother regions of the plot some points were interpolated to produce a regular mesh.

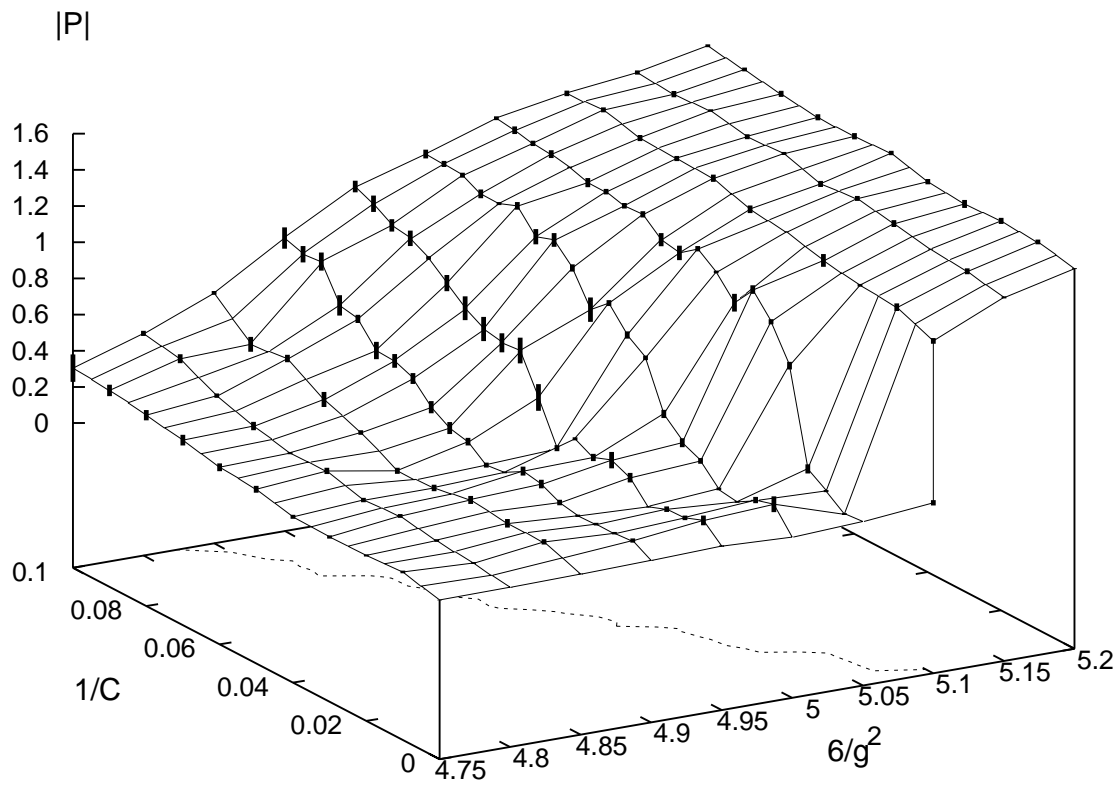


Figure 5: The magnitude of the Polyakov loop in SU(3) as a function of $6/g^2$ and $1/C$. The contour line is where $|P| = 0.5$.

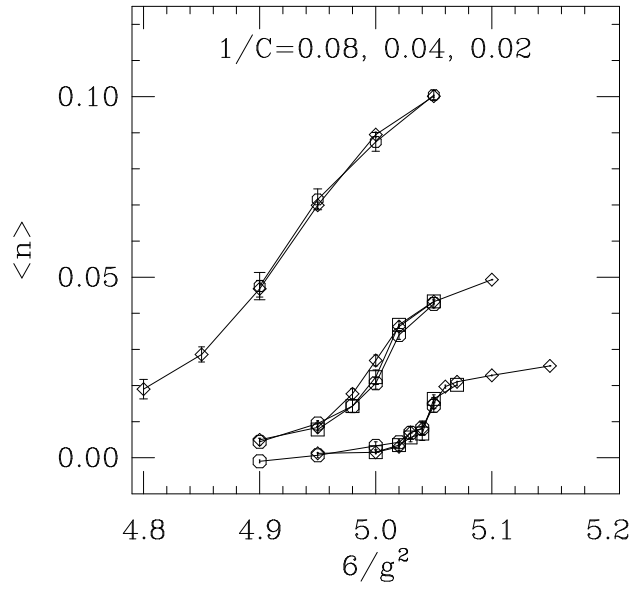


Figure 6: The density as a function of $6/g^2$ on $n_t = 2$ lattices. The curves are, from left to right, $1/C = 0.08$, $1/C = 0.04$ and $1/C = 0.02$. The $1/C = 0.0$ curve is absent because the density is always zero there. The octagons are $6^3 \times 2$ lattices, the squares $8^3 \times 2$ and the diamonds $10^3 \times 2$. The lines just connect the points for each lattice size.

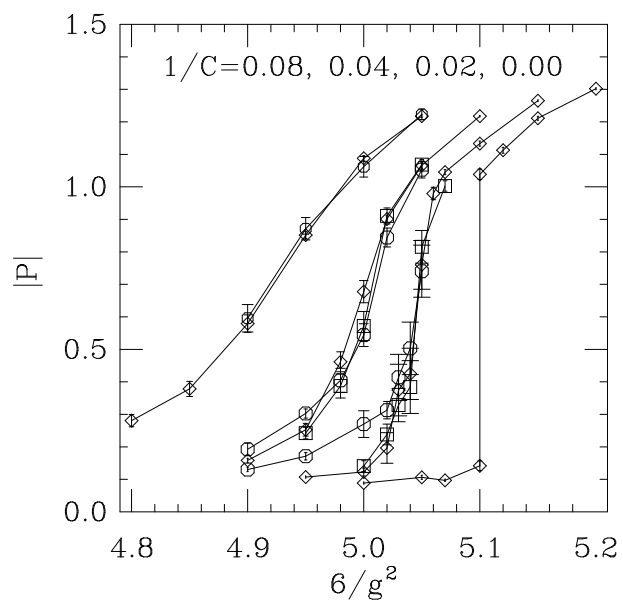


Figure 7: The magnitude of the Polyakov loop averaged over the lattice as a function of $6/g^2$ on $n_t = 2$ lattices. The curves are, from left to right, $1/C = 0.08$, $1/C = 0.04$, $1/C = 0.02$ and $1/C = 0.0$. The meaning of the symbols is the same as in Fig. 6.

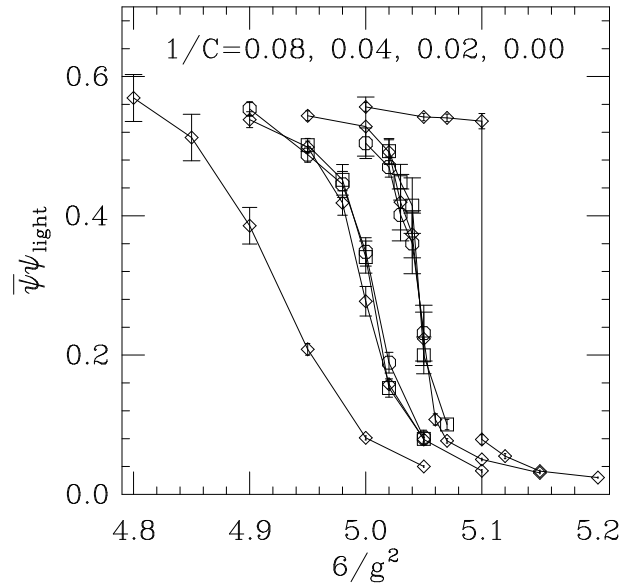


Figure 8: The light quark $\langle \bar{\psi}\psi \rangle$ as a function of $6/g^2$ on $n_t = 2$ lattices. The curves are, from left to right, $1/C = 0.08$, $1/C = 0.04$, $1/C = 0.02$ and $1/C = 0.0$.

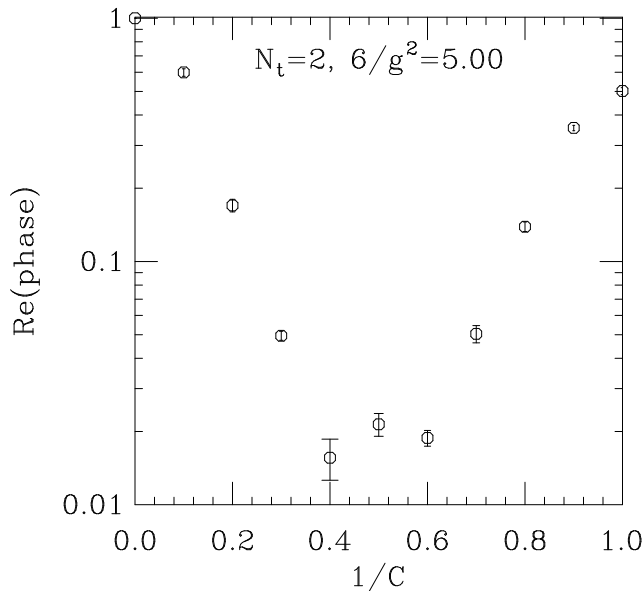


Figure 9: The behavior of $\langle e^{i\theta} \rangle_{||}$ as $1/C$ varies. The lattice size is $6^3 \times 4$ and the gauge coupling is $6/g^2 = 5.0$.

crossover on the spatial size, except for the expected decrease of the Polyakov loop magnitude on cold lattices, we conclude that this rounding is not a finite size effect.

We have also made a series of runs on $6^3 \times 4$ lattices. We began with a series of runs at $6/g^2 = 5.0$. Since the high temperature transition at $1/C = 0$ occurs at $6/g^2 = 5.1$ for $N_t = 2$, this is a fairly cold lattice, with a temperature less than half that for deconfinement at zero density. Fig. 9 shows the behavior of the phase $\langle e^{i\theta} \rangle_{||}$, which in this case gets as small as 0.02. Again, as in SU(2), we find that the light quark $\langle \bar{\psi}\psi \rangle$ remains large for any density at this (cold) value of $6/g^2$, as shown in Fig. 10. At $1/C = 1.0$, the density reaches 1.5 quarks per site, where the quarks have the largest effect on the gauge configurations. In Fig. 11 we show the light quark $\langle \bar{\psi}\psi \rangle$ at $C = 1$ as a function of $6/g^2$, showing the crossover to the chirally symmetric phase as the temperature is raised; while smooth, the crossover is nonetheless quite distinct and at occurs at lower temperature than at zero density.

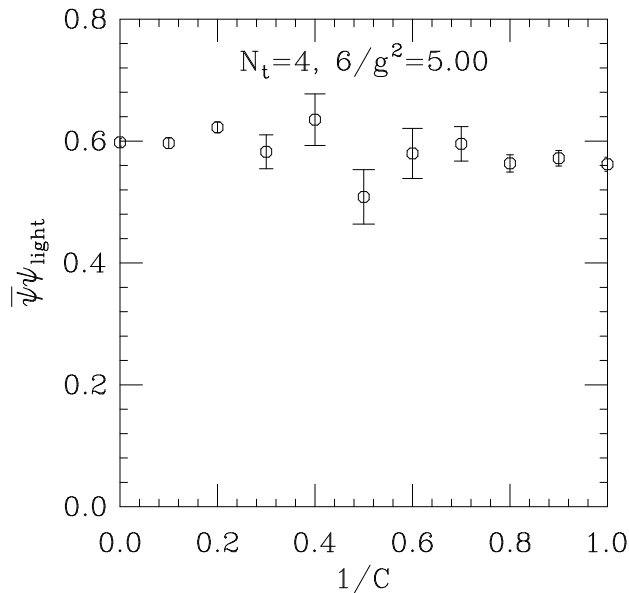


Figure 10: The light quark $\langle \bar{\psi}\psi \rangle$ as a function of $1/C$ on $6^3 \times 4$ lattices, at $6/g^2 = 5.0$.

4 Remarks

Clearly there is much more work to be done in the direction of finite density simulations. In this model, we have not yet addressed the question of whether these results scale in the continuum limit nor tried to extract physical numbers for various quantities. Perhaps the best hope for progress lies in the use of improved actions, with which it may be possible to approach the continuum limit using lattices that are small enough so that the phase problem is no longer hopeless.

The mean field analysis of the Potts model in Ref. [5] showed a disappearance of the phase transition at large density. In the 3d Potts model the first order phase transition persists to some nonzero density (ie. imaginary magnetic field), with a continuously decreasing discontinuity in the order parameter. The hopping parameter expansion in Ref. [6] showed rather smooth behavior of the Polyakov loop and $\langle \bar{\psi}\psi \rangle$ on the chemical potential.

Does the static approximation have anything to do with real QCD? Certainly the nature of the high temperature transition at zero density depends strongly on the presence of dynamical quarks as is becoming clear from large scale simulations of full QCD[9]. However,

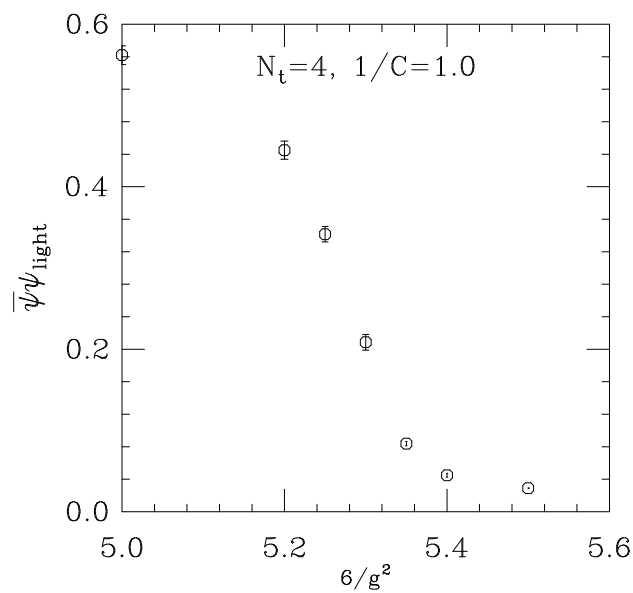


Figure 11: The light quark $\langle \bar{\psi}\psi \rangle$ as a function of $6/g^2$ at $C = 1$ on $6^3 \times 4$ lattices. Recall that the chiral phase transition at zero quark density is at $6/g^2 \approx 5.7$

it is not *a priori* clear to us that a deconfinement transition or chiral symmetry restoration driven by high density should depend on the quarks moving, or whether the mere presence of the quarks would be enough. In particular, we had not expected to see the zero density first order transition disappear for very small quark densities, or for the signal of chiral symmetry restoration to vanish. This suggests that we might want to re-examine the conventional wisdom that a high density of quarks causes a phase transition similar to that caused by high temperature.

Acknowledgements

This work was supported by DOE grant DE-FG03-95ER-40906.

References

- [1] J. Kogut, H. Matsuoka, M. Stone, H.W. Wyld, S. Shenker, J. Shigemitsu, D.K. Sinclair, Nuclear Physics **B225**, 93 (1983); P. Hasenfratz and F. Karsch, Physics Letters **125B**, 308 (1983).
- [2] D. Toussaint, Nuc. Phys. B (Proc. Suppl.) **17**, 248 (1990).
- [3] I.M. Barbour, Nucl. Phys. B (Proc. Suppl.) **26**, 22 (1992).
- [4] A. Hasenfratz and D. Toussaint, Nuc. Phys. B **371**, 539 (1992).
- [5] T.A. DeGrand and C.E. DeTar, Nucl. Phys. **B225[FS9]**, 590 (1983).
- [6] H. Satz, in “*Lattice Gauge Theory: a Challenge in Large-Scale Computing*,” B. Bunk, K.H. Mütter and K. Schilling, eds., Plenum, 1985.
- [7] J. Engels, J. Fingberg, M. Weber, Nucl. Phys. B **332**, 737 (1990).
- [8] K. Kanaya *et al.*, Nuc. Phys. B. (Proc. Suppl.) **26**, 302 (1992).
- [9] F. Karsch, “The phase transition to the quark gluon plasma: recent results from lattice calculations”, (hep-lat/9503010), review talk from “Quark Matter 95”; C. DeTar, “Quark gluon plasma in numerical simulations of lattice QCD”, (hep-lat/9504325), book chapter to appear (R. Hwa, World Scientific).